

# CYBERLEGS - A User-Oriented Robotic Transfemoral Prosthesis with Whole-Body Awareness Control

Luka Ambrožič, Maja Goršič, Joost Geeroms, Louis Flynn, Raffaele Molino

Lova, Roman Kamnik, *Member, IEEE*, Marko Munih, *Member, IEEE*, and Nicola Vitiello, *Member, IEEE*

**Abstract**—Restoring the mobility of transfemoral dysvascular amputees is essential to their rehabilitation process. Impeding this, exhaustion is often the cause of non-effective deambulation of elderly lower-limb amputees using a prosthesis as they use more energy for locomotion than younger amputees do. This article presents finite state control of a novel powered prosthesis prototype for transfemoral amputees based on whole-body awareness. Intention detection was implemented through a non-invasive, distributed wireless wearable sensory system. The CYBERLEGS system was evaluated in a study involving three amputees. The subjects were able to walk with the prosthesis without training, showing accurate performance of the intention detection. The functionality of the CYBERLEGS approach was confirmed by gait pattern analysis and intention detection statistics.

**Index Terms**—Whole-Body Awareness, Finite State Control, Powered Transfemoral Prosthesis, Active Ankle, Wireless Wearable Sensory System, Intention Detection, Amputees.

## I. LOWER-LIMB AMPUTATION AND REHABILITATION

Lower-limb amputation can be a dramatic consequence of severe peripheral arterial disease which is associated with diabetes. It is estimated that 80% of all lower-limb amputations in the US are dysvascular, while about 15% are trauma-related (other causes are cancer or congenital disease). Transfemoral amputation accounts for about a third of all lower-limb amputations. Furthermore, due to higher risk of dysvascular amputation in the elderly, lower-limb amputations are expected to increase as a consequence of population ageing [1]. About 70% of transfemoral amputees use their prosthesis for at least a few hours a day and have an effective deambulation, while 30% do not due to stump-related issues or fatigue from the increased energy cost of walking [2]. A study of Waters et al. [3] looked at the influence of the level of lower-limb amputation on gait and energy expenditure. It

showed that dysvascular transfemoral amputees walked slower (at about 40% of regular gait speed) and consumed 2.5 times more energy than healthy persons. Restoring the mobility of such amputees is an essential element in their rehabilitation process, often achieved by replacing a part of the missing limb by an artificial one.

## II. PROSTHESES AND INTENTION DETECTION

The evolution of lower-limb prostheses through the years culminated in the current use of passive devices, devices with active damping (semi-active or actively-braked prostheses), and powered devices. The majority of modern commercially available passive and semi-active prostheses are able to store energy during initial stance phase and use it to provide push-off in the late stance phase [4]. Powered lower-limb prostheses, capable of producing net power over a gait cycle, were introduced to allow amputees walk with less physical effort and perform other locomotion-related tasks, whose execution was not possible by means of passive or semi-active prostheses (for instance, walking over slopes and climbing/descending stairs). There are a number of research prototypes of active ankle joints [5]–[8] in existence. These may enable a more natural gait pattern during walking as they are able to produce power during every stride. Unlike the ankle, the knee joint dissipates energy during level-ground walking, but produces it when walking on slopes or climbing stairs. Efforts to enable these capabilities resulted in development of active knees [9]–[12] or integrated ankle-knee systems [13]. Despite the promising perspective of powered prostheses their adoption is still quite limited. Current devices have short power autonomy and demand higher cognitive load of the amputee in order to interact with a multi-joint powered device.

Human gait pattern is cyclic and characterized by different phases during which both the knee and the ankle show specific behavior. That is why most control algorithms used in prosthetics and orthotics employ finite state machines [14]. The most important difference between the various control algorithms is the way in which the transitions between phases are detected. Different approaches have been pursued for the development of a reliable interface between the amputee and his or hers powered device. Early ideas pursued echo control, where the prosthetic leg mimicked the kinematics of the sound limb [15]. Some studies relied on the periodical behavior of human gait where the control schemes developed

L. Ambrožič, M. Goršič, R. Kamnik and M. Munih are with the Laboratory of Robotics at the Faculty of Electrical Engineering, University of Ljubljana, Slovenia, E-mail: { luka.ambrozic,maja.gorsic,roman.kamnik,marko.munih}@robo.fe.uni-lj.si.

N. Vitiello is with the BioRobotics Institute, Scuola Superiore Sant'Anna, Pontedera, Italy and the Don Gnocchi Foundation, Florence, Italy. E-mail: n.vitiello@sssup.it

R. Molino Lova is with the Don Gnocchi Foundation, Florence, Italy. E-mail: rmolino@dongnocchi.it

J. Geeroms and L. Flynn are with Vrije Universiteit Brussel, Faculty of Applied Sciences, Dept. of Mechanical Engineering, Brussels, Belgium. E-mail: {jgeeroms,louis.flynn}@vub.ac.be

Manuscript received March 1, 2014. Revised Sept 18, 2014.

for active ankle devices used gait pattern generators (GPGs) [14] to mimic continuous joint behavior. The patterns were adjusted as a function of the stride time and information about the current kinematic/kinetic state. Others investigated user-independent gait classification using mechanical signals such as acceleration measurements at the waist [16], [17] or interaction force and moment measurement between segments of the prosthesis [18]. These studies have been quite successful in user independent classification but required large healthy-subject pools ( $> 50$ ) to create a generic classifier. In some cases, complex surface electromyography (EMG) signals were exploited to direct the movement of individual prosthesis joints. Pattern recognition was utilized to discriminate between the intended motions [19]. Recently, Hargrove et al. published a study where they used nerve transfers and targeted muscle reinnervation (TMR) [20] in combination with EMG decoding to provide control with seamless transitions between the subject's intended movements [21]. However, nerve transfers were performed using a highly invasive surgical procedure at the time of amputation - which is not possible in most amputation cases.

The objective of this article is to present the CYBERLEGS system which comprises a novel 2 degree of freedom (DOF) transfemoral prosthesis with a powered ankle, complemented by a wireless wearable sensory apparatus that acts as a cognitive human-robot interface. It features non-invasive subject-independent intention detection and does not require training of classifiers. The article illustrates how the prosthesis was controlled during level-ground gait by observing a subject's movement and kinetics wirelessly in real-time. Section III presents the major subsystems of the CYBERLEGS system, namely the wearable sensory apparatus, the powered prosthesis [22], and the whole-body awareness control. Movement observation focuses on quiet standing (QS), gait initiation (GI), gait termination (GT), and sub-phases of steady-state gait (SSG) [23]. Results from experimental sessions with three transfemoral amputees are reported and discussed in Section IV. Finally, Section V draws the conclusions.

### III. SYSTEM DESIGN

The EU FP7-ICT-CYBERLEGS project was conceived with the ultimate goal of reducing the energetic and cognitive effort of dysvascular amputees in locomotion-related tasks by means of a novel powered lower-limb prosthesis and orthosis. The prosthesis is complemented by a distributed wearable sensory apparatus tasked with decoding the wearer's intended movement. A conceptual view of the system architecture and human-prosthesis interaction is given in Figure 1.

#### A. Lower-limb prosthesis

The CYBERLEGS  $\alpha$ -prototype prosthesis is an energy-efficient robotic device incorporating an active ankle and a passive knee mechanism. The knee is designed so that it reproduces the level-ground walking joint torque-angle characteristic and the ankle is able to provide the required walking torque. The knee comprises two actuated locking mechanisms that regulate knee stiffness, shown in Figure 2. One provides

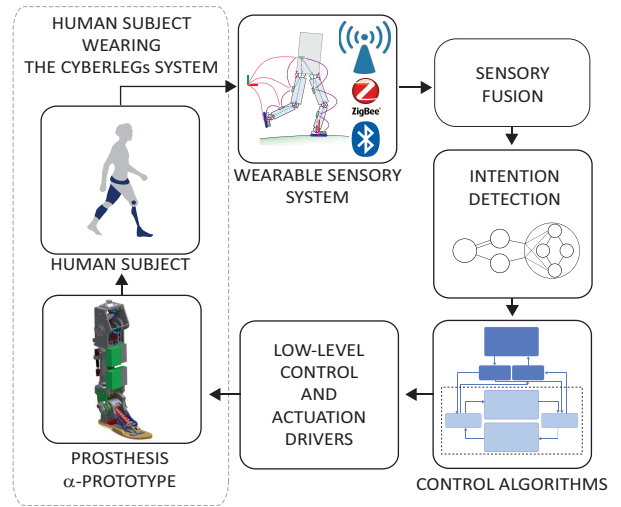


Fig. 1. A conceptual schematic of the CYBERLEGS closed-loop control paradigm. By observing the subject's movement with wireless sensors, the rule-based intention detection algorithm provides the necessary information for the CYBERLEGS control system to move the artificial limb. The prosthesis aims to mimic the subject's natural limb movement patterns, which are, in turn, the feedback information to the intention detection and control algorithms.

additional high stiffness of the knee joint during the weight acceptance phase (Weight Acceptance locking Mechanism - WAM) and the other is used for energetic coupling between the ankle and the knee (Energy Transfer Mechanism - ETM).

The knee characteristic can be divided into three zones with different stiffness profiles: the stiff weight acceptance zone, the flexion zone before toe off and during foot clearance, and the extension zone of the swing phase. During weight acceptance, beginning with heel strike, a stiff spring is locked between the shank and the socket attachment above the knee by means of the WAM ratchet. It provides the necessary high knee stiffness. In late stance the ETM engages automatically when unlocking the WAM. It kinematically couples the knee and ankle joints together before WAM unlocks. Therefore, flexing the knee exerts a force on the ETM cable which is connected to the heel. The same force pulls the heel up, creating a plantar-flexion moment which effectively provides push-off. The knee and ankle joints remain coupled only during the push-off phase. The effect of this mechanism is two-fold: it provides the necessary stiffness at the knee to prevent the amputee from collapsing and transfers the stored energy from the knee to the ankle joint for push-off, making it energy efficient. Once the load is completely shifted to the sound limb, the prosthetic knee stiffness becomes low because the WAM is unlocked and the foot no longer acts on the knee through the ETM. The compressed baseline spring causes flexion of the knee, thus ensuring ground clearance for the swing. The ETM automatically unlocks when the knee reaches a predetermined flexion angle. During the extension period of swing, the knee joint stores negative work from the end of the swing phase in the baseline spring. The WAM ratchet locks the compressed spring into place again which provides the necessary knee stiffness for weight acceptance.

The ankle boasts a new MACCEPA (the Mechanically Adjustable Compliance and Controllable Equilibrium Position

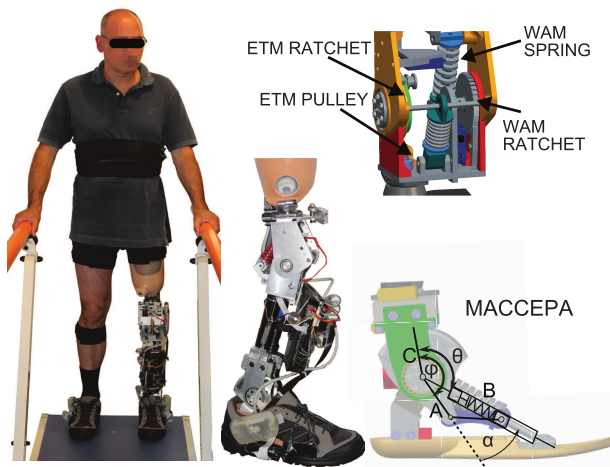


Fig. 2. Left: a subject wearing the  $\alpha$ -prototype of the prosthesis and the wireless sensory system. Right: Close-ups of the prosthetic joints. The prosthesis is an energy-efficient robotic device incorporating an active ankle capable of producing full ankle torque and a passive knee mechanism. It comprises two stiffness regulation locking mechanisms - one that provides high stiffness of the knee joint (Weight acceptance locking mechanism - WAM) and one that determines when the knee and ankle joints are coupled (Energy transfer - ETM).

Actuator) variable compliance actuator [24]. It is compact with variable stiffness and uses a compression spring to achieve the desired stiffening characteristic. The spring pretension was kept constant during trials but can be altered using a motor located in the heel through a non-backdrivable nut. Once it is set it requires no motor power. When the joint is in the rest position, changing the pretension of the spring does not affect the ankle torque. Figure 2 shows the MACCEPA design, but omits the pretension motor, as it is not used during trials. The equilibrium position of the ankle joint is determined by the location of the moment arm of the MACCEPA (A), displaced by an angle  $\varphi$  with respect to the shank (C). The angle  $\theta$  defines the angle of the foot with respect to the shank.  $\alpha$ , the difference between  $\varphi$  and  $\theta$ , defines the torque of the ankle, which increases with the relative displacement of the foot from the moment arm. The torque can be increased by increasing  $\alpha$ , either by changing  $\varphi$ , through motor actuation, or  $\theta$  by changing the position of the foot through the application of an external force. As the magnitude of  $\alpha$  increases, the MACCEPA spring (B) is compressed, allowing the actuator to store energy. The ankle joint angle is considered  $0^\circ$  when the foot's rest position is perpendicular to the shank (at  $\theta^0$ ). The ankle actuator (Maxon RE30 60W DC motor with a 14:1 GP 32 HP planetary gearhead and a 10:1 Graessner D90 hypoid bevel gear) and compliance are designed according to the benchmark criteria of 80 kg individuals walking at a mean speed of 1 stride/s. In terms of mass and inertia, the prosthesis approximately matches those of a normal leg and the prosthetic foot produces pressure loadings on the sole similar to those of a human foot. In the  $\alpha$ -prototype version, power supply, sensory feedback, and control signals are transferred to and from the controller by cables.

### B. Wearable Sensory Apparatus

The CYBERLEGS sensory system uses custom-made components and incorporates wireless pressure-sensitive insoles [25] and an inertial and magnetic measurement system, comprised of 7 autonomous micro electromechanical inertial and magnetic measurement units (IMUs) [26]. The IMUs measure multiple three-dimensional accelerations (range:  $\pm 2g$ ), angular velocities (range:  $\pm 500^\circ/s$ ) and magnetic field (range:  $\pm 1.3Gs$ ). Each IMU consists of an 8-bit microprocessor, individual sensors and a wireless 802.15.4 protocol communication module. The IMUs are small, battery-powered and lightweight devices, having the size of  $(30 \times 20 \times 5)$  mm without the battery. The gyroscopes and accelerometers are calibrated for axis misalignment immediately after assembly while the determination of the bias, misalignment and gain for the magnetometer is performed before experimental trials.

The pressure-sensitive insoles used in this study show high sensitivity to vertical loads and low sensitivity to tangential loads [27]. The insoles measure the vertical ground reaction force ( $f_{GR,v}$ ) and the center of pressure (COP) under the sole. They fit into a size 41-43 (EU) sneaker shoe and do not alter gait or cause discomfort to the wearer. Readings are transmitted over a Bluetooth connection. As explained in [25], the sensing principle of the used pressure sensitive insoles has limitations which impose a systematic error on the force estimate of each sensing element.

In addition to the vertical ground reaction force and center of pressure estimates from the insoles, an unscented Kalman filter [26] is used to fuse the IMU data and assess body segment orientations with respect to the Earth's inertial frame. The sensors provide data to the fusion algorithm at a rate of 100 Hz. Sagittal joint angles are determined from estimated whole-body posture as the differences in orientations between adjacent body segments. Compared to an optoelectronic motion capture system, the difference in accuracy of the system is within  $3^\circ$  [28]. During erect quiet standing, joint angles are set to a joint angle reference of  $0^\circ$ .

### C. Whole-Body Awareness Control

Whole-body awareness control drives the prosthetic knee and ankle through a two-layered hierarchical control system. The low level control is tasked with reading the actuator encoders and controlling the joint and locking mechanism motors in a closed-loop. For the knee joint, the input to the low-level control is a single digital value  $S_{WA}$ , which commands the state of the WAM ratchet motor. For the ankle joint, the low-level PID controller, tuned for the fastest response, tracks the desired equilibrium position of the ankle compliance with respect to the initial offset  $\phi_{MA}^0$  where the foot's rest position is perpendicular to the shank ( $\phi_{MA}^{DES} = \phi_{MA}^0 - \varphi$ ). The high level control sets the desired motor commands for the ankle and knee joints following the recognized activity, namely gait initiation, steady-state gait phases, and gait termination. Recognition of a subject's gait phase in real-time is achieved using a finite state machine with heuristic transition rules. Individual rules refer to raw sensory output from all sensors, fusion estimates and extrapolated functions of the former two.

Whole-body awareness control is implemented in a way that combines the intention detection and finite state control into a single state machine with unified states and transitions.

1) *Intention Detection and Finite State Control*: The high-level intention detection and control is implemented using LabView Statechart Toolbox. States and transitions of the recognition and control state machine (RCSM) are tuned to match states required for finite state prosthesis control. A block diagram of the RCSM transitions and states is shown in Figure 3. At system power-on, the prosthesis is kept rigid with the equilibrium position of the ankle compliance set to zero ( $\phi_{MA}^{DES} = 0^\circ$ ), the knee extended, and the WAM locked. The experimenter must manually enable prosthesis control in order to ensure safety of the subject. Once enabled, state transitions are driven by rules that were developed on the basis of experiments with healthy subjects. Rule threshold values are in large part subject independent. Only rules involving  $f_{GR,v}$  and COP signals require minimal tuning to the subject due to physical differences between them (body weight, foot anatomy). The RCSM discriminates between quiet standing, gait initiation, four steady-state gait phases (prosthetic limb single stance (SS-P), sound limb single stance (SS-S), double stance with prosthesis leading (DS-STS) and with the sound limb leading (DS-PTS)) and gait termination.

2) *Control States and Transitions*: Transitions between states are based on the kinematic patterns of the hip and knee joint angles of both limbs (estimated by 5 IMUs), feet angular velocities (measured by 2 IMUs), and the foot loading patterns (measured by the insoles). Task-independent transition thresholds are based either on raw sensory measurements ( $f_{GR,v}$ , COP, segments' angular velocities) or their extrapolations through sensory fusion (segment orientations and joint angles). Descriptive transition rules are given in Table II along with the control actions of the states for prosthesis control. State/transition labels correspond with those in Figure 3. Input signals and numerical values of the thresholds are described in more detail in [23].

The control can only be enabled or disabled during quiet standing when the WAM is locked and provides the necessary high stiffness of the knee for the support of the amputee. When deactivated, the actuation units are switched off, the WAM remains locked, and the desired equilibrium position of the ankle compliance is set to  $0^\circ$ . For safety purposes, when transitions M or N occur, prosthesis control is paused until the subject movement reaches the gait phase that matches the last active control state. Control resumes if the next transition is an allowed one. In normal operation transitions M and N do

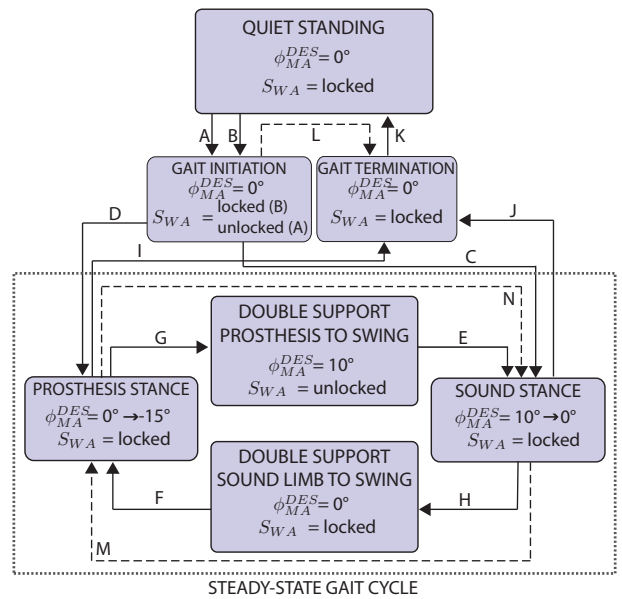


Fig. 3. CYBERLEGS motion observation and high-level control state diagram, showing the recognition and control state machine (RCSM) states and allowed transitions for level-ground walking. Transitions are marked with consecutive letters from A to N. Shown with full-line arrows are the only allowed transitions in normal operation of the prosthesis' control and the dashed-line transitions are allowed only for recognition purposes. The rectangles represent states of the RCSM. They contain state denominations and desired control actions upon entering the state.

not occur.

## IV. EXPERIMENTS WITH AMPUTEES

### A. Subjects

Three unilateral transfemoral amputees participated in the study ( $59.7 \pm 11.0$  years old,  $173.3 \pm 5.8$  cm height,  $60.5 \pm 2.65$  kg weight). Cause for amputation of all three subjects was trauma and all were using the Icelandic-New York (ISNY) socket. All subjects were required to be in good general health apart from missing a limb. The subjects had to have appropriately fitted prostheses of their own and be pain free at the time of recruitment and during experimental sessions. Each subject completed a questionnaire as a part of the Revised Trinity Amputation and Prosthesis Experience Scales (TAPES-R [29]) concerning residual or phantom limb pain and self-rated health and physical capabilities (see Table I). All subjects provided their written informed consent with involvement in the study. The experiments within the research scope of the

TABLE I  
TABLE SHOWS THE SCORES OF THE REVISED TRINITY AMPUTATION AND PROSTHESIS EXPERIENCE SCALES (TAPES-R) CONCERNING RESIDUAL OR PHANTOM LIMB PAIN AND SELF-RATED HEALTH AND PHYSICAL CAPABILITIES.

Participant (ID)	Years since amputation	Use of prosthesis (hours/day)	Experienced residual pain	Experienced phantom limb pain	Self-rated health status	Self-rated physical abilities
Subject 01	10	12	No	Yes	good	good
Subject 02	31	14	Yes	Yes	fair	fair
Subject 03	2.5	14	Yes	Yes	good	good

TABLE II

TABLE SHOWS THE RCSM STATES, LISTS DESCRIPTIVE TRANSITION RULES FOR THE FINITE STATE CONTROL BASED ON WHOLE-BODY AWARENESS AND GIVES THE CONTROL ACTIONS FOR THE PROSTHETIC KNEE AND ANKLE.

State / Transition	Transition allowed when detected:	Ankle Control	Knee Control
A (QS $\rightarrow$ GI with prosthetic limb)	hip flexion of prosthetic limb lateral weight transfer to the sound limb	$\phi_{MA}^{DES} = 0^\circ$	WAM unlocked
B (QS $\rightarrow$ GI with the sound limb)	flexion of sound limb lateral weight transfer to the prosthetic limb	$\phi_{MA}^{DES} = 0^\circ$	WAM locked
Gait initiation (GI)		$\phi_{MA}^{DES} = 0^\circ$	No action
L			No action
C	only sound foot is loaded flexion in the joints of prosthetic leg		No action
Sound stance (SS-S)		after 300 ms $\phi_{MA}^{DES} \rightarrow 0^\circ$	WAM unlocked for 300 ms
D	only prosthetic foot is loaded flexion in the joints of sound leg		No action
Prosthesis stance (SS-P)		$\phi_{MA}^{DES} \rightarrow -15^\circ$ with a slope of $-25^\circ/s^1$	WAM locked
G	sound foot loading under the heel prosthetic foot loading under the toes hip flexion over threshold		No action
Double Support - Prosthesis To Swing (DS-PTS)		$\phi_{MA}^{DES} \rightarrow 10^\circ$	WAM unlocked
N	only sound foot is loaded flexion in the joints of prosthetic leg		No action
E	only sound foot is loaded flexion in the joints of prosthetic leg		No action
H	prosthetic foot loading under the heel sound foot loading under the toes hip flexion over threshold		No action
Double Support - Sound Limb To Swing (DS-STs)		$\phi_{MA}^{DES} = 0^\circ$	WAM locked
M	only prosthetic foot is loaded flexion in the joints of sound leg		No action
F	only prosthetic foot is loaded flexion in the joints of sound leg		No action
J	both feet in contact with the ground slow foot movement upright body posture feet loading starts to distribute symmetrically		No action
I	refer to transition J		No action
K	stand still in double support upright body posture symmetric feet loading		No action
Gait termination (GT)		$\phi_{MA}^{DES} \rightarrow 0^\circ$	WAM locked

project were approved by the Ethical Committee of the Don Gnocchi Foundation.

### B. Experimental Setup and Protocol

The measurement system consisted of a walkway with handrails and the CYBERLEGS system. The CYBERLEGS

<sup>1</sup>Positive angle causes a dorsiflexion torque and a negative value a plantarflexion torque.

system comprised the  $\alpha$ -prototype robotic prosthesis connected with a socket, a gurney with power management components and a cognitive control unit (National Instruments Compact-RIO with field-programmable gate array (FPGA) capability). Additionally, the system incorporated the CYBERLEGS wearable sensory apparatus: one insole was worn by the subject, the other fitted on the prosthetic limb. Six IMUs were attached on lower extremity segments (thighs, shanks, feet) using soft, elastic straps with silicone lining to prevent slipping. One IMU was placed near the lumbosacral joint on

the back. Sensory data processing and fusion algorithms ran on a dedicated real-time PC controller (xPC Target real-time operating system). The two controllers were connected through a local network (LAN) and data was transferred using user datagram protocol (UDP). Analog synchronization was used to monitor latencies of the data transfer between controllers.

The subjects were requested to perform a minimum of twenty 6-meter-long walks with the prosthesis at their preferred speed and step length. The protocol allowed them to familiarize themselves with the prosthesis in five to ten test walks prior to the start of the experimental session. This gave the investigators an opportunity to fine-tune subject-specific parameters based on weight, height and side of the amputated limb. All subjects were asked to perform a number of trials where they initiated their gait with the prosthetic or healthy limb, respectively, while they could terminate their gait per their preference (with the healthy or prosthetic limb). Subject 01 completed only 15 trials, due to a temporary WAM malfunction. Subjects 02 and 03 accomplished 25 trials each. Subject 03 was available for experiments for two consecutive days and thus completed an additional experimental session.

### C. Data Collection and Analysis

Each trial was documented using a camera. The data were recorded at a rate of 100 Hz. With a combination of expert knowledge and supervised automated protocols, the gait data were segmented offline into phases. The investigators compared the offline-segmented data to the phase detection data recorded online in order to evaluate the accuracy of the algorithm. The detection accuracy was evaluated as the success ratio between the number of correctly recognized phases and the number of all actual instances of a particular phase during the trial.

Maximal loads during stance phases were evaluated for each limb in order to show loading differences between the healthy leg and the prosthesis. Furthermore, the impulse of force  $I_F$  of the stance phase for each individual limb was evaluated, using (1),

$$I_F = \int_{t_{HS}}^{t_{TO}} f_{GR,v}(t) dt \quad (1)$$

where  $t_{HS}$  and  $t_{TO}$  denote the start (heel strike) and end (toe off) time of an individual stance phase, and  $f_{GR,v}$  the vertical ground reaction force of the stance limb. Impulse of force describes the action of a force profile in a given time interval and gives insight into load distribution over an entire stance phase of each leg. This adds an additional dimension to the asymmetry assessment since it also captures the temporal distribution of feet loading.

### D. Safety

All amputees walked between parallel bars so they could support their weight by using their arms in case of any failure of the prosthetic device. A physiotherapist oversaw the tests and was ready to physically support the amputees whenever it was requested. Additionally, a safety loop was implemented in the control system, that: i) allowed the knee joint to be

unlocked - and then flexed - only when the sound limb actually touched the ground, ii) locked the knee and set the desired equilibrium position of the ankle compliance to  $0^\circ$  in order to provide stable support whenever an error with the incoming information from the recognition algorithms was detected. Moreover, the experimenter had the possibility to switch off the power at any time.

## V. RESULTS AND DISCUSSION

Experimental results show the capability of the user to interact with the prosthesis without a long, cognitively demanding training. The effect of whole-body awareness prosthesis control on the movement of the amputees is discussed with regard to recorded gait patterns. Intention detection accuracy is evaluated and analysis of results provides insight into the quality of the restored gait pattern. Effects of false intention detection on control are presented.

### A. Gait pattern

Figure 4 shows example cases of four types of trials where the amputees initiated gait with the sound limb (GI-S, Figure 4a), terminated gait with the sound limb in stance and the prosthesis in swing (GT-S, Figure 4b), initiated gait with the prosthesis (GI-P, Figure 4c), and terminated gait with the prosthetic limb in stance and the sound limb in swing (GT-P, Figure 4d). The top two graphs show the vertical ground reaction forces ( $f_{GR,v}$ ) and the recognized phase, respectively. The bottom two graphs show how the recognized phases influence the movement of the knee and ankle joint of the prosthesis. In particular, the second graph from the bottom shows healthy and prosthetic knee joint angles, estimated by the inertial system, and the state of the weight acceptance locking mechanism (WAM). The bottom graph shows, for the prosthetic ankle joint, the reference value ( $\phi_{MA}^{DES}$ ) and real position ( $\phi_{MA}$ ) of the ankle compliance equilibrium, and the prosthetic ankle joint angle. The difference in real and desired equilibrium position of the ankle compliance is due to a slow motor driver, despite optimal tuning of the low-level controller. The grey areas demonstrate the detection of initiation and termination with each of the limbs. Each of the four examples also includes at least one full SSG cycle. Figure 4 illustrates how the actions of the prosthetic knee and ankle correspond to each of the detected gait phases.

1) *Gait Initiation and Steady-State Gait:* During initiation with the sound limb, the prosthetic limb is in single stance and the ankle joint prepares for the push off (Figure 4a).  $\phi_{MA}^{DES}$  is gradually decreased to provide stiffness and push-off torque. When double support is detected, the prosthesis prepares for swing ( $T1$ ).  $\phi_{MA}^{DES}$  is then set to a positive angle to allow foot clearance when the amputee fully transfers his weight on the sound limb. Just before the prosthetic limb goes to swing, the WAM unlocks. During swing extension the WAM locks ( $T2$ ) and the knee can freely move in only one direction as a result of the locked WAM ratchet. Once the prosthetic limb swings and the knee extends, the ankle plantar-flexes in preparation of foot strike. In double support, the amputee transfers weight from the healthy to the prosthetic limb ( $T3$ ). As a result

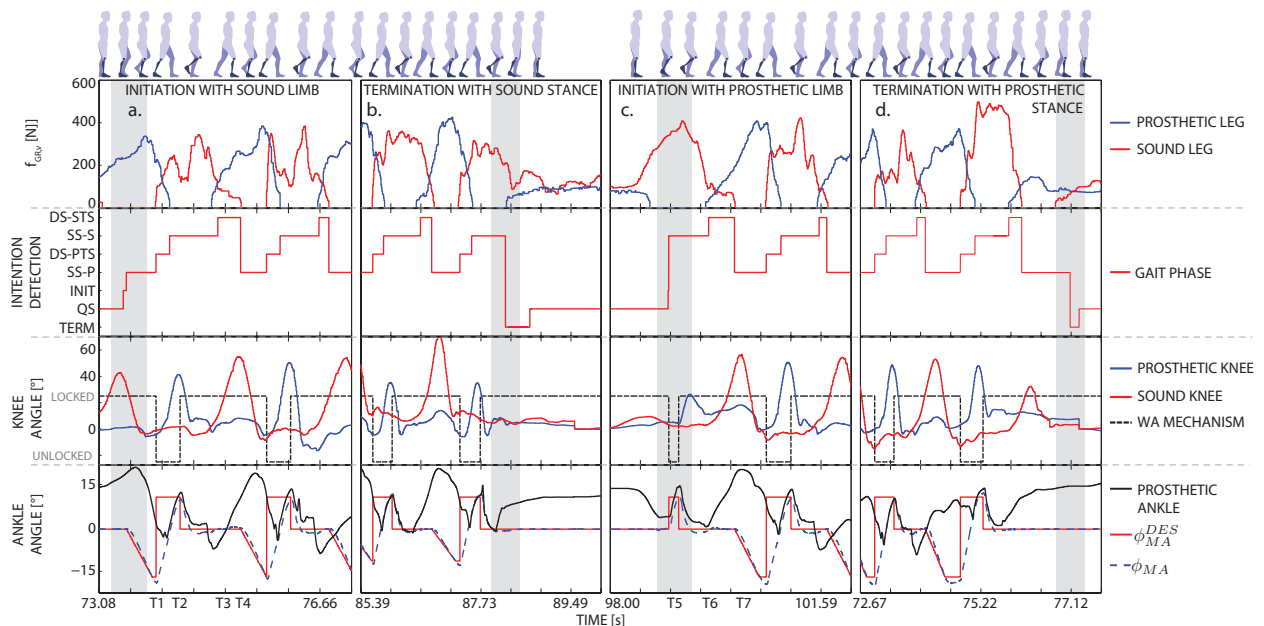


Fig. 4. Example cases for four different types of transitions (gait initiation with the sound limb of Subject 02 (a.), gait termination with the sound limb in stance of Subject 03 (b.), gait initiation with the prosthesis of Subject 02 (c.), and gait termination with the prosthetic limb in stance of Subject 01 (d.). From top to bottom the figure shows ground reaction forces -  $f_{GR,v}$ , recognized phases, knee variables (joint angles and the state of the weight acceptance mechanism (WAM)), and ankle variables (the desired equilibrium position ( $\phi_{MA}^{DES}$ ) of the MACCEPA compliance, its real position ( $\phi_{MA}$ ), and the prosthetic ankle joint angle). Marked with a grey background are the featured initiation and termination events. Human body figures above the graphs indicate the pose in a given phase with featured sound and prosthetic limb.

of forward movement, the prosthetic ankle flexes under the weight because of the compliance of the MACCEPA.  $\phi_{MA}^{DES}$  remains at  $0^\circ$  and the WAM remains locked to provide support. At  $T4$  the gait cycle is concluded and the same behavior is repeated in the next cycle. During SSG, the joint trajectories for both the healthy and the prosthetic knee are similar which indicates effective mimicking of the healthy knee kinematic pattern by the prosthesis. When initiating with the prosthetic limb (Figure 4c), the WAM unlocks when gait initiation is recognized and the knee flexes because of a compressed spring. 300ms later the WAM ratchet locks in preparation for the initial prosthesis stance. In sound limb single stance ( $T5$ ), the ankle dorsi-flexes in order to allow foot clearance during swing. When the knee locks, the ankle flexes again and remains in the rest position ( $\phi_{MA}^{DES} = 0^\circ$ ) until prosthetic foot strike. The compliance of the MACCEPA allows the ankle joint to flex when the amputee is transferring load from the heel towards the front of the foot (between  $T6$  and  $T7$ ).

2) *Gait Termination*: Two examples of gait termination are presented (final single stance of the sound limb - Figure 4b and final single stance of the prosthesis - Figure 4d). Termination is considered a terminal double stance. When termination in either case is detected, the knee remains stiff and the WAM does not unlock like in double support (DS-PTS). The equilibrium position of the ankle elasticity stays at  $0^\circ$ .

### B. Intention Detection

Figure 5 presents the statistics of recognition success for gait initiation, gait termination and four SSG phases by the RSM.

Each bar indicates the success rate for a given subject-session-phase combination. The number of successful recognitions (S), the total number of phases performed by a subject (N), the individual subject-phase recognition success rate (%), and the overall success rate for a given phase are given in line with the bar for each subject-session combination. The bars are grouped in clusters where each of the clusters represents one of the phases.

Overall, the initiation recognition of the intention detection algorithm was accurate in 85.2% of the cases. The success rate for SSG phases was 96.9%. Detection of sound leg single stance phase performed with the highest mean success rate across all subjects (99.7%). Considering that the intention detection algorithm was developed on the basis of healthy subjects, the high success rate implies that the loading pattern and kinematic parameters of the sound leg were similar to those of healthy subjects. Detection of double stance - sound limb to swing phase exhibited the lowest success rate. In this phase, amputees had to transfer weight from the sound to the prosthetic limb and this indicates that they did not have sufficient trust in the prosthesis. Furthermore, adaptation to the new prosthesis was observed for Subject 03 (S03), who completed two sessions. Success ratios improved from SESSION1 to SESSION2 for all phases which involved the prosthetic leg stance (SS-P, DS-PTS, DS-STs). This implies higher confidence of walking with the prosthesis of the subject.

All subjects could terminate gait with either the sound or the prosthetic limb. Recognizing gait termination is challenging since gait can be terminated asymmetrically. The termination of gait is defined as the transition from steady-state gait to quiet standing, with no discrimination between symmet-

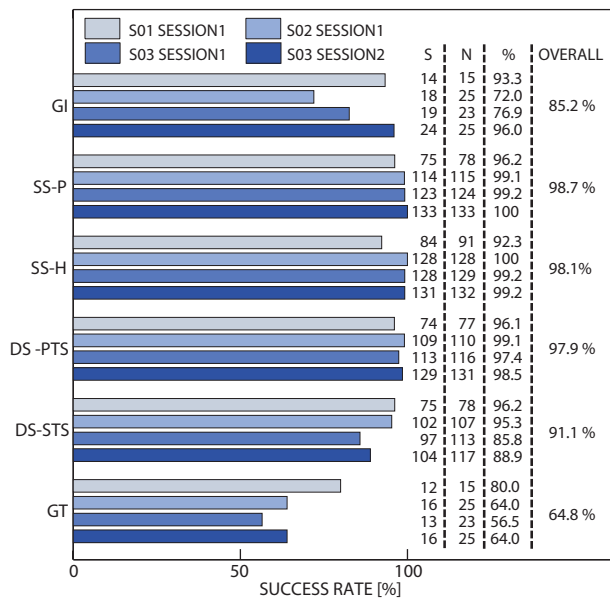


Fig. 5. Recognition success rates of gait initiation (GI), SSG phases (sound limb single support (SS-S), prosthetic limb single support (SS-P), double support with sound limb to swing (DS-PTS)), and double support with the prosthesis to swing (DS-ST), and gait termination (GT). Each bar shows recognition success for each subject-session-phase combination. S denotes the number of successful recognitions of a phase, N the total number of the phase instances, % the success rate for each subject-session-phase combination and the final column the overall success rate for each phase.

rical and asymmetrical termination. Based on experiments with healthy subjects, we found that most healthy gaits end symmetrically (with equally distributed load on both limbs), therefore termination detection was developed on this premise. When subjects terminated gait in an unexpected manner (i.e., asymmetrically), the gait ended in asymmetric quiet standing (the load was predominantly on the sound limb). We did not observe this behavior in healthy subjects. Results from experiments with amputees have shown that we need to account for these termination cases in our intention detection algorithm. Nevertheless, the success of the GT recognition (64.8%) was evaluated with regard to the total number of terminations performed by the subject (symmetric, asymmetric or irregular). Moreover, the success rate of GT recognition for cases where the subject terminated gait symmetrically was 85.1%. Based on the overall GT recognition success rate we can induce that the termination detection is the weakest part of the recognition algorithm.

### C. Symmetry in Ground Reactions

The top graph in Figure 6 shows average durations of the steady-state gait phases in successfully recognized strides of the amputees. The bar plot has four clusters, one for every subject-session combination.

Steps performed after the initiation of gait and prior to its termination are taken into account. Figure 6 shows how all subjects relied more on the healthy limb during SSG, spending more time in SS-S than in SS-P. Double support durations appear equal for both double support combinations which indicates a smooth and natural-like walking pattern. The

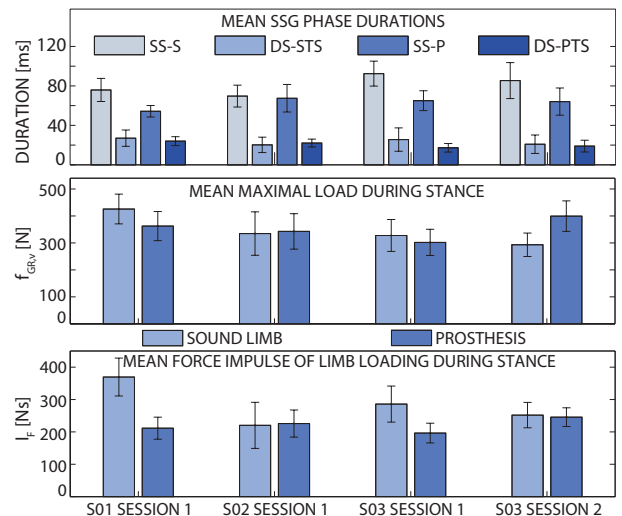


Fig. 6. Gait characteristics and symmetry in stance loading. For each subject-session combination, the top graph illustrates a mean duration of each of the four steady-state walking gait (SSG) phases, the middle graph shows the maximal load and the bottom graph the load impulse of both limbs when they were in contact with the ground.

bottom two graphs in Figure 6 show the mean maximal insole load by the sound and prosthetic limb, and the mean force impulse of limb loading during stance phases of both limbs, respectively, for all subject-session combinations. Focusing on the middle graph, we can observe that Subject 01 (S01 SESSION1) and Subject 03 (S03 SESSION1) put more load on the healthy limb during SESSION1 while Subject 02 (S02 SESSION1) loaded both limbs equally. However, if we inspect the limb loading during the second session of Subject 03, we can observe that the subject loaded the prosthetic limb more than during the first session. This indicates that the subject placed more trust in the prosthesis during the second session. In the bottom graph of Figure 6, both temporal and amplitude characteristics are captured for the limb loadings. The impulse of force during stance reveals asymmetry in limb loading, showing that the subjects generally put more weight on the healthy limb and loaded the limb for a greater period of time compared to the prosthetic limb. If we closely examine the graphs for both sessions of Subject 03, we can infer that the subject adapted his loading pattern to the prosthesis in SESSION2. While the impulse of force for the second session of Subject 03 indicates that the gait was more symmetrical, the duration of limb stances did not greatly alter. However, the loading of the prosthetic limb did increase. In general, the subjects did not alter the timing of their gait pattern with use. We suspect this is due to lack of feedback information from the prosthetic limb, because the subjects could not anticipate future activities by the prosthesis. Therefore they felt safer with their sound limb firmly in contact with the ground.

### D. Effect of False Recognitions on Control

Transition detection is critical for prosthesis control as it ensures accurate and robust state transitions. If the detection is inaccurate, the control may trigger inappropriate actions of the prosthesis, which can disturb the dynamics and stability

of the wearer during locomotion. However, variability in the amputees' locomotion pattern makes designing robust transition rules difficult. If the rules are too unrestrictive, a transition may always occur but may happen at an inappropriate moment. On the other hand, if the rules are too restrictive, the transition might not occur at all. Real-time intention detection and pattern recognition is frequently affected by misclassifications. No intention detection system has yet been reported to be 100% accurate. In any case, the effects of erroneous detection must be mitigated. Otherwise unintended prosthesis movements may cause users to become frustrated and be unsuccessful at the task they are trying to complete. The prosthesis controller design required all the phases of the gait cycle to be performed in appropriate order to successfully complete the control sequence of the given gait cycle. Otherwise, only detection of gait termination could end the control sequence. For example, if the detected phase was in accordance with the order of the gait cycle, the control was enabled; otherwise the control was paused and the prosthesis remained extended with a locked knee until the motion observation triggered a transition to continue the gait cycle, thus mimicking the operation of a passive prosthesis. In this way, unpredicted and possibly unsafe behavior of an active prosthesis was prevented.

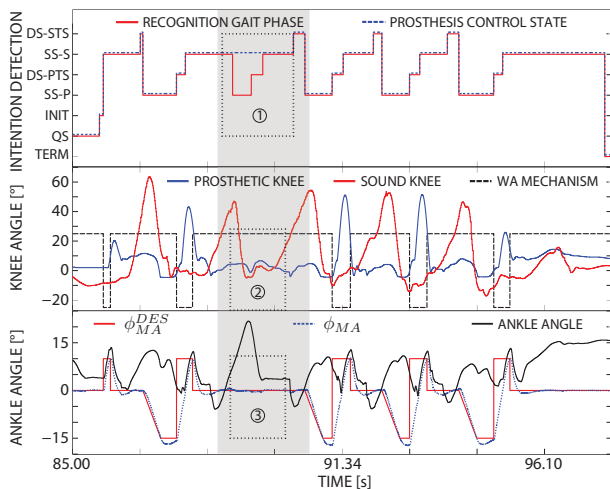


Fig. 7. An example case of an unsuccessful detection during gait of Subject 02. Marked in grey is the part of the trial, where the DS-ST5 gait phase was not detected. Areas of interest are marked with a dashed rectangle and each is denoted with a number. Rectangle (1) shows where the control of the prosthesis became paused, rectangle (2) shows the area where the WAM should normally unlock and the prosthetic knee flex, and rectangle (3) shows the area where the ankle joint remained passive without adding energy to the gait. The top graph shows the recognized gait phase in red and the blue dashed line shows the corresponding control state of the prosthesis. The middle graph shows the consequence of the paused control on the knee joint. Marked in red is the sound knee joint angle, in blue the prosthetic knee joint angle, and the dashed line shows the state of the WAM. For the ankle joint, the bottom graph features the prosthetic ankle joint angle in black, the desired equilibrium position of the MACCEPA compliance ( $\phi_{MA}^{DES}$ ) in red, and the actual equilibrium position of the compliance ( $\phi_{MA}$ ) with a blue dashed line.

Figure 7 shows an example of an unsuccessful detection for Subject 01. Marked in grey is the part of the trial, where one transition did not occur, which paused the control of the prosthesis. Once the transition occurred during the next gait cycle, control of the prosthesis resumed. In this situation the

knee WAM remained locked with the ankle compliance set at the equilibrium position of a flat foot ( $\phi_{MA}^{DES} = 0^\circ$ ), prepared for the heel strike during the next stance phase. The amputee subjectively reported to perceive this as if wearing a regular passive prosthesis with a locked knee. This meant that the amputees had to perform an unnatural swing, which introduced a change into the gait pattern. The swing required more effort from the amputee than with regular control, mostly due to the length of the prosthesis during swing. However, a fault in detection did not unbalance the amputee, and supported walking resumed after the next regular stride pattern was detected.

## VI. CONCLUSION

This article presents the CYBERLEGS system which comprises an actuated ankle, a passive knee with knee-ankle energy transfer and a pervasive wearable sensory system. Experimental evaluation of the system was performed in order to validate the whole-body awareness control of an active transfemoral prosthesis. The system was worn by three amputees during level-ground walking. Finite-state control of the prosthesis was driven by a simple rule-based movement recognition algorithm which relied solely on information from non-invasive wireless sensors. The intention detection performed accurately enough to allow closed-loop control of the prosthesis with a human in the loop. Suitable operation of the prosthesis was demonstrated by the feet loading pattern and knee joint kinematics. The subjects were able to walk with the prosthesis without previous training and the subject who completed two sessions improved his gait pattern during the second session. This study suggests that whole-body awareness can be used for intention detection and control without the need for large training datasets. The proposed control concept is simple, does not require machine learning and the structure of the system allows quick adaptation to the user in order to ensure a positive user experience. In the future, the prosthesis will be upgraded with a fully active knee in order to allow the amputees to perform additional maneuvers, such as stair negotiation and walking on slopes.

## ACKNOWLEDGMENT

This work was supported by the European Commission 7th Framework Program as part of the CYBERLEGS project under grant No. 287894, by the Slovenian Research Agency (ARRS) under grant No. P20228, and by a PhD grant of the Agency for Innovation by Science and Technology Flanders (IWT). The authors would like to thank Federica Vannetti and Guido Pasquale from Fondazione don Carlo Gnocchi, Florence, Italy for their contributions in realization of the experiments. Special thanks go to the participating amputees.

## REFERENCES

- [1] P. L. Ephraim, T. R. Dillingham, M. Sector, L. E. Pezzin, and E. J. MacKenzie, "Epidemiology of limb loss and congenital limb deficiency: a review of the literature," *Archives of physical medicine and rehabilitation*, vol. 84, no. 5, pp. 747–761, 2003.
- [2] T. Pohjolainen, H. Alaranta, and M. Kärkäinen, "Prosthetic use and functional and social outcome following major lower limb amputation," *Prosthetics and orthotics international*, vol. 14, no. 2, pp. 75–79, 1990.

- [3] R. Waters, J. Perry, D. Antonelli, and H. Hislop, "Energy cost of walking of amputees: the influence of level of amputation." *The Journal of bone and joint surgery. American volume*, vol. 58, no. 1, p. 42, 1976.
- [4] B. J. Hafner, J. E. Sanders, J. M. Czerniecki, and J. Ferguson, "Transtibial energy-storage-and-return prosthetic devices: a review of energy concepts and a proposed nomenclature," *Journal Of Rehabilitation Research And Development*, vol. 39, pp. 1–11, 2002.
- [5] J. K. Hitt, R. Bellman, M. Holgate, T. G. Sugar, and K. W. Hollander, "The SPARKy (Spring Ankle with Regenerative Kinetics) project: Design and analysis of a robotic transtibial prosthesis with regenerative kinetics," in *Proceedings of the ASME 2007 International Design Engineering Technical Conferences & Computers and Information in Engineering Conference IDETC/CIE 2007, Las Vegas, Nevada, USA, 2007*, pp. 1587–1596.
- [6] P. Cherelle, V. Grosu, A. Matthys, B. Vanderborght, and D. Lefeber, "Design and Validation of the Ankle Mimicking Prosthetic (AMP-) Foot 2.0," *Neural Systems and Rehabilitation Engineering, IEEE Transactions on*, vol. PP, no. 99, p. 1, 2013.
- [7] S. Au and H. Herr, "Powered ankle-foot prosthesis," *IEEE Robotics & Automation Magazine*, vol. 15, no. 3, pp. 52–59, 2008.
- [8] R. D. Bellman, M. a. Holgate, and T. G. Sugar, "SPARKy 3: Design of an active robotic ankle prosthesis with two actuated degrees of freedom using regenerative kinetics," *2008 2nd IEEE RAS & EMBS International Conference on Biomedical Robotics and Biomechanics*, pp. 511–516, 2008.
- [9] A. O. Kapti and M. S. Yucenur, "Design and control of an active artificial knee joint," *Mechanism and Machine Theory*, vol. 41, no. 12, pp. 1477–1485, Dec. 2006.
- [10] E. C. Martinez-Villalpando and H. Herr, "Agonist-antagonist active knee prosthesis: a preliminary study in level-ground walking," *Journal of Rehabilitation Research & Development*, vol. 46(3), no. 3, pp. 361–374, 2009.
- [11] F. Sup, A. Bohara, and M. Goldfarb, "Design and control of a powered knee and ankle prosthesis," in *Robotics and Automation, 2007 IEEE International Conference on*. IEEE, 2007, pp. 4134–4139.
- [12] Ossur. (2014, February) [www.ossur.com](http://www.ossur.com). [Online]. Available: <http://www.ossur.com>
- [13] F. Sup, A. Bohara, and M. Goldfarb, "Design and Control of a Powered Transfemoral Prosthesis," *International Journal of Robotics Research*, vol. 27, no. 2, pp. 263–273, 2008.
- [14] R. Jimenez-Fabian and O. Verlinden, "Review of control algorithms for robotic ankle systems in lower-limb orthoses, prostheses, and exoskeletons," *Medical engineering & physics*, vol. 34, no. 4, pp. 397–408, 2012.
- [15] W. Flowers and R. Mann, "An electrohydraulic knee-torque controller for a prosthesis simulator," *Journal of biomechanical engineering*, vol. 99, no. 1, pp. 3–8, 1977.
- [16] L. Kilmartin, R. K. Ibrahim, E. Ambikairajah, and B. Celler, "Optimising recognition rates for subject independent gait pattern classification," in *Signals and Systems Conference (ISSC 2009), IET Irish*. IET, 2009, pp. 1–6.
- [17] N. Wang, E. Ambikairajah, B. G. Celler, and N. H. Lovell, "Accelerometry based classification of gait patterns using empirical mode decomposition," in *Acoustics, Speech and Signal Processing, 2008. ICASSP 2008. IEEE International Conference on*. IEEE, 2008, pp. 617–620.
- [18] H. Varol and M. Goldfarb, "Real-time intent recognition for a powered knee and ankle transfemoral prosthesis," in *Rehabilitation Robotics, 2007. ICORR 2007. IEEE 10th International Conference on*, June 2007, pp. 16–23.
- [19] A. J. Young, L. H. Smith, E. J. Rouse, and L. J. Hargrove, "A comparison of the real-time controllability of pattern recognition to conventional myoelectric control for discrete and simultaneous movements," *Journal of neuroengineering and rehabilitation*, vol. 11, no. 1, p. 5, 2014.
- [20] T. A. Kuiken, G. Li, B. A. Lock, R. D. Lipschutz, L. A. Miller, K. A. Stubblefield, and K. B. Englehart, "Targeted muscle reinnervation for real-time myoelectric control of multifunction artificial arms," *Jama*, vol. 301, no. 6, pp. 619–628, 2009.
- [21] L. J. Hargrove, A. M. Simon, A. J. Young, R. D. Lipschutz, S. B. Finucane, D. G. Smith, and T. A. Kuiken, "Robotic leg control with emg decoding in an amputee with nerve transfers," *New England Journal of Medicine*, vol. 369, no. 13, pp. 1237–1242, 2013.
- [22] J. Geeroms, L. Flynn, R. Jimenez-Fabian, B. Vanderborght, and D. Lefeber, "Ankle-knee prosthesis with powered ankle and energy transfer for cyberlegs  $\alpha$ -prototype," in *Rehabilitation Robotics (ICORR), 2013 IEEE International Conference on*. IEEE, 2013, pp. 1–6.
- [23] M. Goršič, R. Kamnik, L. Ambrožič, N. Vitiello, D. Lefeber, G. Pasquini, and M. Muih, "Online phase detection using wearable sensors for walking with a robotic prosthesis," *Sensors*, vol. 14, no. 2, pp. 2776–2794, 2014. [Online]. Available: <http://www.mdpi.com/1424-8220/14/2/2776>
- [24] R. Van Ham, B. Vanderborght, M. Van Damme, B. Verrelst, and D. Lefeber, "Maccepa, the mechanically adjustable compliance and controllable equilibrium position actuator: Design and implementation in a biped robot," *Robotics and Autonomous Systems*, vol. 55, no. 10, pp. 761–768, 2007.
- [25] S. Crea, M. Donati, S. M. M. De Rossi, C. M. Oddo, and N. Vitiello, "A wireless flexible sensorized insole for gait analysis," *Sensors*, vol. 14, no. 1, pp. 1073–1093, 2014.
- [26] T. Beravs, P. Reberšek, D. Novak, J. Podobnik, and M. Muih, "Development and validation of a wearable inertial measurement system for use with lower limb exoskeletons," in *Humanoid Robots (Humanoids), 2011 11th IEEE-RAS International Conference on*. IEEE, 2011, pp. 212–217.
- [27] D. Novak, P. Reberšek, S. M. M. De Rossi, M. Donati, J. Podobnik, T. Beravs, T. Lenzi, N. Vitiello, M. C. Carrozza, and M. Muih, "Automated detection of gait initiation and termination using wearable sensors," *Medical engineering & physics*, vol. 35, no. 12, pp. 1713–1720, 2013.
- [28] S. Šlajpah, R. Kamnik, and M. Muih, "Kinematics based sensory fusion for wearable motion assessment in human walking," *Computer methods and programs in biomedicine*, vol. 166, no. 2, pp. 131–144, 2014.
- [29] P. Gallagher, F. Franchignoni, A. Giordano, and M. MacLachlan, "Trinity amputation and prosthesis experience scales: a psychometric assessment using classical test theory and rasch analysis," *American Journal of Physical Medicine & Rehabilitation*, vol. 89, no. 6, pp. 487–496, 2010.

**Luka Ambrožič** received his university diploma in Electrical Engineering from University of Ljubljana, Slovenia, in 2012. Immediately after he joined the Laboratory of Robotics at the Faculty of Electrical Engineering, University of Ljubljana as a researcher. His research interests are human biomechanics, autonomous devices and bionics.

**Maja Gorišič** received her university diploma in Electrical Engineering from University of Ljubljana, Slovenia, in 2012. She soon joined the Laboratory of Robotics at the Faculty of Electrical Engineering, University of Ljubljana as a researcher. She is currently active in the field of intention detection and human biomechanics.

**Joost Geeroms** obtained his Master's degree from the Vrije Universiteit Brussel (VUB) in 2011. He is currently a Ph.D. student at VUB under supervision of Prof. Dirk Lefeber. His research is centered on actuated prosthetics.

**Louis Flynn** received his M.S. degree in Mechanical Engineering from Michigan State University in 2009. He is currently a PhD student at the Vrije Universiteit Brussel developing actuated prostheses and exoskeletons.

**Dr. Raffaele Molino Lova** is a cardiologist and cardiac surgeon. He is a senior researcher and assistant scientific director involved in the clinical management of the Cardiac Rehabilitation Unit of the Fondazione don Gnocchi, Center of Florence. His research interests are in the fields of exercise physiology, ventilatory gas exchange kinetics and energy cost of walking.

**Roman Kammik** received his D.Sc degree in Electrical Engineering from the University of Ljubljana, Slovenia, in 1999. He is currently an Associate Professor with the Laboratory of Robotics at Faculty of Electrical Engineering, University of Ljubljana. In the past, he was a visiting researcher at the University of Glasgow, Department of Mechanical Engineering, Great Britain, and at the University of Alberta, Faculty of Medicine and Oral Health Sciences, Department of Biomedical Engineering, Canada. His research interests are focused on biomedical engineering and robotics.

**Marko Munih** received the B.Sc., M.Sc. and D.Sc. Degrees in electrical engineering from the University of Ljubljana, Slovenia, in 1986, 1989 and 1993, respectively. He is a Professor and Head of Laboratory of Robotics at the Faculty of Electrical Engineering, University of Ljubljana. His research interests lie in functional electrical stimulation of paraplegic lower extremities, biomechanics, haptic interfaces and rehabilitation engineering. In the past, he was a Research Assistant with the Implanted Devices Group in the Department of Medical Physics and Bioengineering at University College London and Royal National Orthopaedic Hospital Trust, Stanmore, UK, where he did research on unsupported standing of paraplegics and development of a sensory amplifier. Currently, he leads the research group for Analysis and synthesis of human and machine motion at the University of Ljubljana.

**Nicola Vitiello** Nicola Vitiello received the M.Sc. degree in biomedical engineering (cum laude) from the University of Pisa, Italy, in 2006, and from Scuola Superiore Sant'Anna (SSSA), Pisa, Italy, in 2007. He received his Ph.D. degree in biorobotics from the SSSA, in 2010. He is currently an Assistant Professor with The BioRobotics Institute, SSSA, where he leads the Wearable Robotics Laboratory. His research interests include the development of wearable robotic devices for human motion assistance and rehabilitation, and robotic platforms for neuroscientific investigations.